Fast Wavelet Transform Algorithms for Sonar Signal Analysis

Limin Yu and Fei Ma
Xi'an Jiaotong-Liverpool University, Suzhou, China
Email: {limin.yu, fei.ma}@xjtlu.edu.cn

Langford B. White
The University of Adelaide, Adelaide, Australia
Email: lang.white@adelaide.edu.au

***Abstract*—In active sonar, received echoes are composed of multiple replicas of transmitted sonar signal with time delays and attenuations through multipath. In non-stationary scenarios, different multipath also exhibits different scaling. This phenomenon provides a way to explicitly resolve the multipath components given the availability of a rational orthogonal wavelet (ROW) analysis framework. This paper establishes the ground work of a wavelet-based multipath resolving structure by tackling the fast wavelet transform (FWT) filter bank (FB) design for ROWs. A review of different FWT algorithms in terms of scaling, translation and computational complexity is presented. The proposed FWT FB design for ROWs enables practical applications of the multipath/Doppler resolving structure in both active and passive sonar signal analysis. A simplified model for active sonar signal multipath resolving is presented to demonstrate the multipath resolving mechanism.**

***Index Terms*—fast wavelet transform, sonar signal analysis, multipath, rational orthogonal wavelet, wavelet filter banks**

I. Introduction

In sonar signal analysis, estimate of multipath delays serves the purposes of multipath cancellation, beam forming, and target localisation/tracking [1], [2], [3]. For scenarios that the platform (either the target or the receiver, or both) is moving, different multipath signals exhibit different time delays and scaling [4], [5]. An accurate estimation of the scale factors, therefore, enables a separation of multipath components. More importantly, the resolved multipath components are expected to be combined in an array processing context to improve sonar target detection and tracking [6], [7].

For active sonar, a natural solution to resolve the multipath in terms of multipath delays and scales in motion settings, is to use wavelet pulse (at the transmitter) and wavelet analysis (at the receiver). The wavelet analysis decomposes the sonar echoes and localises the multipath signal into specific orthogonal wavelet subspaces and time instants. Most fast algorithms to calculate the wavelet analysis parameters are based on dyadic wavelets. The scale dilation factor is $\alpha = 2^j$. However, in sonar systems, the wavelet scales resolution that one is expected to achieve is much finer in order to distinguish the multipath components. The scale resolution is expected to be less than $\Delta = 10^{-2}$ which is hard to achieve by most of the fast wavelet analysis tools.

In the literature, various wavelet analysis algorithms were proposed with different resolution and computational complexity. The reader is referred to section II for a review of these algorithms. Among them, rational orthogonal wavelet (ROW) is a prospective solution with a fractional dilation factor $\alpha = \frac{q+1}{q}, q \in Z^+$. The scale resolution is $\Delta = \frac{1}{q}$ approximately. The mathematical definition of the ROW family could be found in [8] and [9].

In this paper, the authors focus on the derivation of fast wavelet transform (FWT) algorithm for ROWs. The fast algorithm is then applied to active sonar to demonstrate the multipath resolving with ROW filter banks (FBs).

The paper is organized in the following. Section II summarizes wavelet transform algorithms with different scale resolutions and translations. Section III details the FWT for ROWs based on rational sampling filter bank (FB). A simplified example for active sonar multipath resolving is presented in section IV. Section V presents the conclusion.

II. Review of Fast Wavelet Transform Algorithms with Different Resolutions

Based on the original continuous wavelet transform (CWT) [10], [11], fast wavelet transforms were developed with different time/scale resolution and computational complexity to meet specific requirements on signal analysis.

The continuous wavelet transform of a signal $f(t)$, $t \in R$ is defined by

$$W_\psi f(\alpha,\tau) = \frac{1}{\sqrt{\alpha}} \int f(t)\psi^*(\frac{t-\tau}{\alpha})dt, \alpha \in R^+ - \{0\}, \tau \in R \quad (1)$$

Manuscript received July 20, 2013; revised November 20, 2013.

doi: 10.12720/ijsps.1.2.183-189

where $\psi(t)$ is the wavelet basis function, α is the scale factor, τ is the translation factor, $*$ represents complex conjugate, and $W\psi f(\alpha, \tau)$ are the wavelet coefficients.

Direct computation of continuous wavelet transform (CWT) requires $O(N^2)$ operations per scale. With FFT-based fast convolution algorithm, the computational complexity reduces to $O(N \log(N))$ per scale.

As a special case of CWT, FWT algorithms were developed to calculate wavelet coefficients at discrete scale and translations. The famous Mallat's FWT algorithm [10] is defined under the framework of dyadic multiresolution analysis (MRA). It calculates discrete wavelet transform (DWT) for orthogonal/biorthogonal wavelets at dyadic scales $\alpha = 2^j$ and dyadic translations $\tau = k\alpha, j, k \in Z$. Its computational complexity is a global $O(N)$ based on perfect reconstruction filter banks.

Based on different discretisation of the scale and translation factors, the àtrous FWT algorithms [12] were proposed with dyadic scale $\alpha = 2^j$ and integer translations $\tau = k, j, k \in Z$. In comparison, B-spline-based FWT [13] has an integer scale α = j, and integer translations $\tau = k, j, k \in Z$. The computational complexity is $O(N)$ per scale for both FWT algorithms. It is worth noting that the algorithms have an octave or an integer scale resolution, which might not be adequate for applications requiring a finer scale resolution.

To obtain a finer scale resolution, Shensa's FWT algorithms [14] were developed for discretised scale and translation

$$\alpha = 2^{J+\frac{m}{M}}, \tau = k2^j, j, k \in Z, m = 0, \cdots, M-1, M \in Z^+$$

where m is called the 'voice'. It gets a finer resolution per octave and the computational complexity is M times of the octave-by-octave algorithm. A more detailed comparison of Mallat, à trous and Shensa's wavelet transform was given in [15].

Another octave-based FWT algorithm with finer scale resolution is the general spline-based FWT. It calculates wavelet coefficients at $\alpha = 2^{\frac{j}{Q}}, \tau = k, j, k \in Z, Q \in Z^+$. The computational complexity is O (N) per scale. Notice that for Q = M , the two algorithms have the same scale resolution which is equivalent to the dilated scales $a_0^j, a_0 = 2^{\frac{1}{Q}} = 2^{\frac{1}{M}}$. If the discretisation parameters M or Q are selected properly, these algorithms would be able to approximate a CWT, i.e., to calculate wavelet coefficients at an arbitrary scale, and therefore were termed as fast CWT algorithms in the literature.

To achieve a global $O(N)$ computational complexity and finer resolution to approximate the CWT, one of the solutions is the rational orthogonal wavelet (ROW) based on the framework of rational MRA (a), where $\alpha = \frac{q+1}{q}, q \in Z^+$. The FWT algorithm is implemented via rational sampling wavelet analysis/synthesis FBs. It is similar to Mallat's FWT but with a finer scale resolution $\alpha = a^j, 1 < a < 2$. An illustration of the scale resolution of different FWT algorithms is given in Fig.1. Table I gives a brief summary of these algorithms.

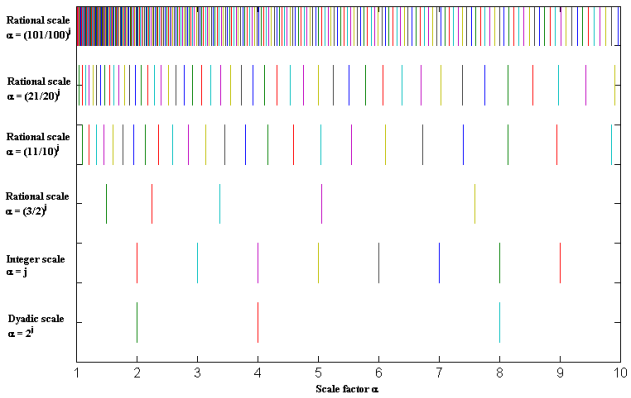

Figure 1. A comparison of different resolution

III. FWT FOR RATIONAL ORTHOGONAL WAVELET (ROW)

In this section, a detailed description of the FWT for ROWs is presented. As proven in [9], the ROWs have compact support in the frequency domain and are infinite in the time domain. Therefore, there is no FIR solution of the analysis/synthesis filters for the FWT. The fast algorithm, however, is available that is implemented in the frequency domain as shown in [16] or by FIR-based approximation as the derivation of discrete Meyer (dMeyer) wavelet from Meyer wavelet [17]. Both frequency-domain and time-domain FWT algorithms are described in this section with a focus on the design of time-domain tree structured FWT algorithms. The computational complexity for real-time implementation of the FWT is also analysed.

A. Frequency-Domain FWT Algorithm for ROWs

In Baussaud's paper [16], the fast algorithm for real ROWs was given and implemented in the frequency domain. The corresponding pyramid synthesis and analysis algorithms for the real valued wavelets with $a = \frac{p}{q} = \frac{q+1}{q}$ are shown in Fig. 2 and Fig. 3. The lowpass filters are computed by

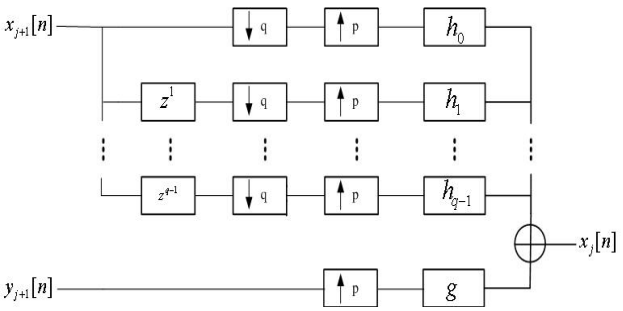

Figure 2. Synthesis filter bank of real rational orthogonal wavelet $(a = \frac{p}{q}, p = q+1)$

TABLE I. A COMPARISON OF CWT AND DWT ALGORITHMS

Scale and Translation	Algorithm	Computational Complexity
$\alpha \in R^+ - \{0\}, \tau \in R$	CWT	$O(N^2)$ per scale; $O(N\log(N))$ per scale with FFT
$\alpha = 2^j, \tau = k\alpha, j,k \in Z$	Mallat's FWT	Global $O(N)$
$\alpha = 2^j, \tau = k, j,k \in Z$	àtrous's FWT	$O(N)$ per scale
$\alpha = j, \tau = k, j,k \in Z$	àtrous's FWT; B-spline-based FWT	$O(N)$ per scale
$\alpha = 2^{j+\frac{m}{M}} = a_0^j, \tau = k2^j, a_0 = 2^{\frac{1}{M}}$, $j,k \in Z, m = 0,\cdots,M, M \in Z^+$	Shensa's FWT	Global $O(MN)$
$\alpha = 2^{j/Q} = a_0^j, \tau = k, a_0 = 2^{\frac{1}{Q}}$, $j,k \in Z, Q \in Z^+$	Spline-based FWT	$O(N)$ per scale
$\alpha = 2^j, \tau = q\alpha, a = (q+1)/q$, $q \in Z^+, j \in Z$	Aucher's rational MRA; Baussard's FB	Global $O(N)$

$$H_n(\omega) = \sqrt{a}\,\frac{\Phi(a\omega)}{\Phi(\omega)} e^{-ina\omega} \tag{2}$$

where $\Phi(\omega)$ is the Fourier transform of the scaling function $\phi(t)$, and $n = 0, \bullet\bullet\bullet, q-1$. The highpass filters are given by

$$G(\omega) = \sqrt{a}\,\frac{\Psi(a\omega)}{\Psi(\omega)} \tag{3}$$

where $\Psi(\omega)$ is the Fourier transform of the wavelet function $\varphi(t)$.

Notice that $Hn(\omega)$ and $G(\omega)$ are used which are also denoted as $H_n(e^{j\omega})$ and $G(e^{j\omega})$ for discrete filters. The filters are of infinite length in the time domain, therefore the pyramid algorithm in [16] was implemented in the frequency domain in order to take advantage of the definition of filters in the frequency domain. However, the time domain FB algorithm might be preferable to the block-by-block algorithm in the frequency domain for delay sensitive applications.

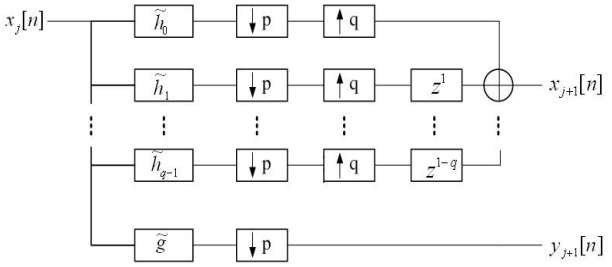

Figure 3. Analysis filter bank of real rational orthogonal wavelet $(a = \frac{p}{q}, p = q+1)$.

B. Time-domain FWT Algorithm for ROWs

In this section, a FIR approximation of the fast analysis and synthesis algorithm is proposed. The algorithm is not restricted to the perfect reconstruction property but with a fidelity that suits communications applications.

Following the FB construction for dyadic Meyer wavelet as shown in [17], we give the example of FB construction for a RROW with q = 2 and $a = \frac{q+1}{q} = \frac{3}{2}$, denoted by $\varphi^{(\frac{3}{2})}(t)$. The filters h_n [n] and g[n] are constructed by synchronous sampling of the continuous filters $h_n(t)$ and $g(t)$, which are numerically constructed based on their definition in the frequency domain. The lowpass and highpass synthesis filters $h_0[n]$, h_1[n] and g[n] are shown in Fig. 4. Note that to conform to the spectrum of the continuous filters $h_n(t)$ and $g(t)$, the sampling rate f_s is selected to be greater than or equal to the Nyquist rate,

$$f_s^{Nyquist} = \frac{\omega_3}{\pi} = a^2\,\frac{\omega_1}{\pi} \tag{4}$$

$$= q+1+\frac{q+1}{2q+1} \tag{5}$$

$$\approx q+\frac{3}{2} \tag{6}$$

The constructed filters h_0 [n], h_1 [n] and g[n] are related to a redundant multiresolution analysis (MRA) structure of a frame [18] $\{\varphi^{(a)}_{b_0;j,k}(t) := a^{\frac{j}{2}}\varphi(a^j t - kb_0), a = \frac{3}{2}, b_0 = f_s\}$, rather than a R-wavelet [18] $\{\varphi^{(a)}_{1;j,k}(t) := a^{\frac{j}{2}}\varphi(a^j t - k), a = \frac{3}{2}, b_0 = 1\}$. This redundancy leads to the shift-invariance property of the FB which is closely related to the issue of synchronisation for communication applications [5].

The validity of the tree-structured FWT algorithm could also be verified by the convergence of the iteration of the synthesis filters [19]. Based on the two-scale relation of the rational MRA(a) as shown in equations (2) and (3), there are

$$\Phi(a\omega) = a^{-(\frac{1}{2})} H_n(\omega) e^{jna\omega}\Phi(\omega) \tag{7}$$

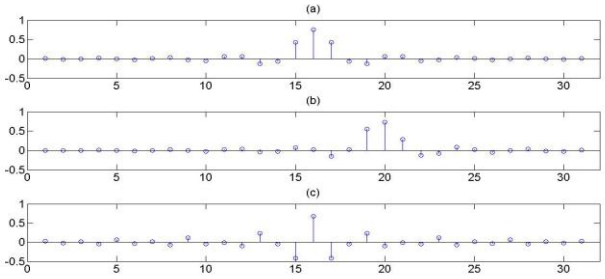

Figure 4. Synthesis filters h0, h1, g for real rational orthogonal wavelet (a=3/2, (a) filter h0, (b) filter h1, and (c) filter g.

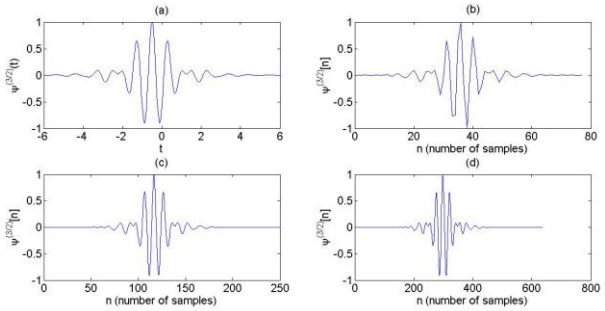

Figure 5. Convergence of iterated FB to the wavelet function, (a) wavelet function $\varphi^{(\frac{3}{2})}(t)$, (b) output of 2 iterations, (c) output of 4 iterations, and (d) output of 6 iterations

$$\Psi(a\omega) = a^{-(\frac{1}{2})} G(\omega)\Phi(\omega) \tag{8}$$

Therefore, the wavelet function can be generated by

$$\Psi(\omega) = a^{-(\frac{1}{2})} G(a^{-1}\omega)\Phi(a^{-1})$$

$$= a^{-(\frac{1}{2})} G(a^{-1}\omega)\prod_{k=2}^{\infty}\{a^{-(\frac{1}{2})} H_n(a^{-k}\omega)e^{jna-(k-1)\omega}\}\Phi(0)$$

where $\Phi(0)=1$. Based on the filters shown in Fig. 4, the wavelet basis function $\varphi^{(\frac{3}{2})}(t)$ can be generated by the iteration of *g* and h_0 *(n = 0)*, or *g* and h_1 *(n = 1)*. Fig. 5 shows the comparison of the RROW function $\varphi^{(\frac{3}{2})}(t)$ and the output of 2, 4, and 6 iterations of the constructed synthesis filters. The resemblance of the wavelet function and iteration outputs demonstrates good convergence of the tree-structured FWT.

C. Simplified Tree-Structured FWT FB

The synthesis/analysis FBs shown in Fig. 2 and Fig. 3 can be further simplified into 2-branch FBs based on the observation of the strong resemblance of Baussard's FB and Jelena and Vetterli's rational sampling PR FB of the direct design method [20]. The connection between the two FBs provides a method to simplify Baussard's FB by replacing the parallel lowpass FB with a single branch. On the other hand, the knowledge of Baussard's FB gives a solution to the design of rational sampling FB based on the rational orthogonal wavelet.

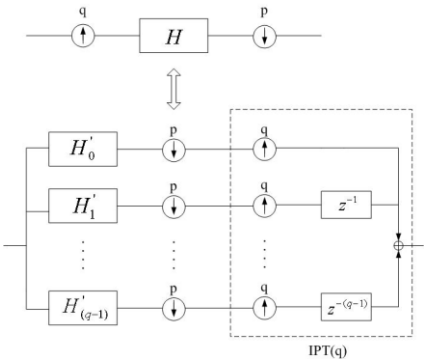

Figure 6. Direct design of rational sampling FB.

The direct design method proposed in [20] is based on the equivalent FB structures shown in Fig. 6. It transforms a single branch with upsampling by *q* and downsampling by *p* to a *q* channel analysis bank with downsampling by *p* and an inverse polyphase transform of size *q* (IPT(*q*)), assuming *q* and *p* are coprime and *q* > *1*. The filters in the *q*-channel analysis bank are defined by

$$H_i^{'}(z) = z^{d_i} H_{t_i}^{(v)}(z) \tag{9}$$

where $d_i = \left\lfloor \frac{pi}{q} \right\rfloor$. The operator $\lfloor x \rfloor$ returns the largest integer not greater than x. The integer number t_i is the modulus of $\frac{pi}{q}$, $t_i = \mathrm{mod}(pi, q)$. Functions $H_0^{(v)}, \cdots, H_{q-1}^{(v)}$ are the polyphase components of *H* with respect to *q*. The rational sampling FB design problem is reduced to finding a perfect reconstruction structure for a q-channel FB, with design constraints imposed on filters $H_0^{(v)}, \cdots, H_{q-1}^{(v)}$.

The above relations between the single branch rational sampling filter H and the parallel FB $H_i^{'}$ can be utilized directly to simplify Baussard's FB by replacing the parallel lowpass filters h_n, n = 0, • • • , q − 1 in Fig. 2 with a single branch of filter with rational sampling factor p/q as shown in Fig. 6. The equivalent filter H is derived as

$$\begin{aligned} H(z) &= H_0(z^q) + z^{-(1+p+q)} H_0(z^q) + \cdots + z^{-(q-1)(1+p+q)} H_0(z^q) \\ &= (1 + z^{-(1+p+q)} + \cdots + z^{-(q-1)(1+p+q)} H_0(z^q)^{'} \\ &= A(z^{(1+p+q)}) H_0(z^q)^{'} \end{aligned} \tag{10}$$

where $A(z) = 1 + z^{-1} + z^{-2} + \cdots + z^{-(q-1)}$. The filter $H_0(z)$ is given by equation (2) with n = 0. The derivation is presented in the Appendix A.

The connection between the two FBs shown in Fig. 2 and Fig. 6 also gives a solution to the design of rational sampling FB with sampling factor of *p/q*, *p = q+1*, based on the rational orthogonal wavelet with scale factor of *a=p/q=1+1/q*. The nature of the continuous WT/IWT FBs forms the basis of PR and shift-invariance (SI) properties of the designed rational sampling FB. The PR

property is verified immediately based on the definition of wavelet transform pair. The shift-invariant property of the iterated FB can be examined by evaluating the two-scale relation of the wavelet lowpass filters $\tilde{h}_i$ and the highpass filter g proposed in [16]:

$$a_{j,sq+i} = \sum_r \tilde{h}_i[ps-r]a_{j-1,r} \quad (11)$$

$$d_{j,n} = \sum_r \tilde{g}[pn-r]a_{j-1,r} \quad (12)$$

Shifting the approximation and detail coefficients by 1, there are

$$a_{j,(s-1)q+i} = \sum_r \tilde{h}_i[ps-r]a_{j-1,r-p} \quad (13)$$

$$d_{j,(n-1)} = \sum_r \tilde{g}[pn-r]a_{j-1,r-p} \quad (14)$$

which infer that a delay of 1 at stage j means a delay of for the input signal. Therefore, the FBs shown in Fig. 2 and Fig. 3 have the SI property.

D. Computational Complexity

Based on the FWT algorithm proposed in section III-C, the computational complexity of FWT for ROW FBs can be evaluated. The computational complexity has the order of

$$O(N + Na^{-1} + Na^{-2} + \cdots Na^{-(J-1)}) \quad (15)$$

$$= O((q+1)(1-a^{1-J})N \quad (16)$$

$$= O((q+1)N) \text{ as } J \to \infty \quad (17)$$

where a is the scale factor. Therefore the computational complexity of FWT for the ROW FBs increases when the value of q increases or when a is getting closer to 1.

IV. A Simplified Model for Multipath Resolving with FWT

Given the FWT FB algorithm derived in section III, this section uses a simplified multipath model to illustrate the resolving of two multipath by the ROW FB. The scale factor of the designed FB is $a = 201/200$. The transmitted signal is only distorted by two multipath with delay and attenuation. The model is given as

$$y(t) = \rho_1\psi(a^{m_1}(t-\tau_1)) + \rho_2\psi(a^{m_2}(t-\tau_2)) \quad (18)$$

where $\psi(t)$ is the transmitted signal, $y(t)$ is the received signal, ρ_i, τ_i, m_i are the attenuation, time-delay and scaling at the i-th multipath, $i = 1, 2$, and $m_1 > m_2$.

If normalising the multipath signal based on the first arrival, and assuming the target is approaching the detector, the received signal is expressed as

$$\bar{y}(t) = \psi(t) + \rho\psi(a^{-m}(t-\tau)) \quad (19)$$

where $0 < \rho < 1$ and $m \in Z^+$. Assuming the direct path has a length of D and the second path has a length of L, there is $L > D$. The first multipath has a scale factor of 1. The second multipath signal has a scaling factor of $\alpha = D/L = a^{-m}$. The normalised attenuation factor is $\rho = D/L = \alpha$. The multipath time T_M is defined as τ. Assuming $m = 2$, the FB that covers the scale range of $\{m = -2, -1, 0, 1, 2, 3, 4, 5\}$. The FB outputs are illustrated in Fig. 7. For a situation that the multipath $T_M = \frac{1}{2}\tau$, there is $\alpha = D/L = a^{-1}$. The FB outputs are shown in Fig. 8. The multipath is resolved in both time and scale domain as the two emissions are localised in different subbands with different time shifts as shown in Fig. 7 and Fig. 8.

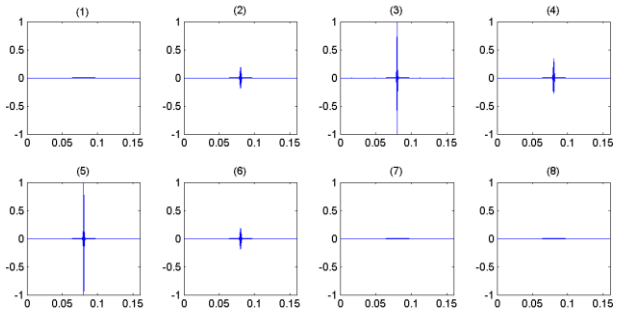

Figure 7. Simplified scenarios with two multipath with wavelet signaling $\psi_a = \frac{201}{200}(t)$

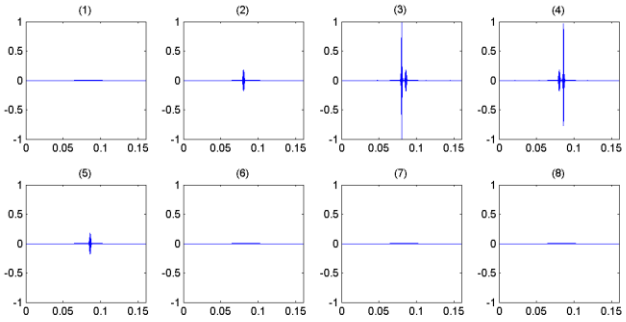

Figure 8. Simplified scenarios with two multipath with wavelet signaling $\psi_a = \frac{201}{200}(t)$ (less delay between two multipath).

V. Conclusion

The paper proposes a time-domain design of fast wavelet transform (FWT) filter banks (FBs) for the rational orthogonal wavelet (ROW) family. The availability of the FWT algorithm facilitates practical applications of the ROWs in data communication and sonar detection. Notice that the FIR approximation of the wavelet analysis/synthesis filters prevents the wavelet transform and its perfect reconstruction (PR) and shift invariance (SI) properties to be exact. However the PR and SI properties hold with high fidelity based on the good convergence of the FIR approximation to the continuous wavelet transform. As shown in section IV,

resolving of multipath is demonstrated using a ROW FB with scaling factor of $a = \frac{q+1}{q}$, q =200. The multipath signals are resolved illustratively, but not precisely in the scale domain. Based on the preliminary result, a more realistic geometrical channel model will be used to test the multipath resolving performance in both active and passive sonar.

VI. Appendix A Derivation of Simplified Row Analysis FB

Let us start from the direct rational sampling FB design method in [20]. The filters in the equivalent q-channel analysis FB were given in equation (20), and quoted herein,

$$H_i^{'}(z) = z^{d_i} H_{t_i}^{(v)}(z) \tag{20}$$

Considering the special case of $p = q + 1$, the definition is equivalent to

$$H_i^{'}(z) = z^{i} H_i^{(v)}(z) \tag{21}$$

where $i = 0, \bullet\bullet\bullet, q - 1$. The polyphase expression of the equivalent filter H in the single branch is

$$H(z) = H_0^{(v)}(z^q) + z^{-1} H_1^{(v)}(z^q) + \cdots + zq^{-1} H_{q-1}^{(v)}(z^q) \tag{22}$$

The resemblance of the FBs in Fig. 2 and Fig. 6 infers the relation that

$$\tilde{H}_i(z) = z^{i} \tilde{H}_i^{(v)}(z) \tag{23}$$

where $\tilde{H}_i(z)$, $i = 0, \bullet\bullet\bullet, q - 1$ are the filters in the rational orthogonal analysis FB in Fig. 2. $\tilde{H}_i^{(v)}(z)$, $i = 0, \ldots, q - 1$ are the polyphase components of $\tilde{H}$ with respect to q. The filter $\tilde{H}$ is the equivalent single branch filter we seek, and can be expressed by

$$\tilde{H}(z) = \tilde{H}_0^{(v)}(z^q) + z^{-1} \tilde{H}_1^{(v)}(z^q) + \cdots + zq^{-1} \tilde{H}_{q-1}^{(v)}(z^q) \tag{24}$$

Based on the definition of $\tilde{H}_i(z)$ in equation (2), there is

$$\tilde{H}_i(z) = z^{-ai} \tilde{H}_0(z), \; i = 0, \cdots, q - 1 \tag{25}$$

Substituting (25) into (24), we have

$$\tilde{H}(z) = \tilde{H}_0(z^q) + z^{-(1+p+q)} \tilde{H}_0(z^q) + \cdots + z^{-(q-1)(1+p+q)} \tilde{H}_0(z^q) \tag{26}$$

Defining $A(z) = 1 + z^{-1} + z^{-2} + \cdots + z^{-(q-1)}$, the equivalent filter $\tilde{H}$ is expressed as

$$\tilde{H}(z) = A(z^{(1+p+q)}) \tilde{H}_0(z^q) \tag{27}$$

References

[1] J. S. Abel and K. Lashkari, "Track parameter estimation from multipath delay information," *J. Ocean Engineering*, vol. 12, pp. 207–221, 1987.

[2] B. Friedlander, "Accuracy of source localization using multipath delays," *IEEE Trans. Aerospace and Electronic Systems*, vol. 24, pp. 346–359, 1988.

[3] Q. Chen, W. Xu, X. Pan, and J. Li, "Wideband multipath rejection in synthetic aperture sonar imaging," *IET Radar, Sonar, Navigation*, vol. 3, pp. 620–629, 2009.

[4] M. Johnson, L. Freitag, and M. Stojanovic, "Improved doppler tracking and correction for underwater acoustic communications," in *Proc. IEEE Conf. Acoustics, Speech, Signal Processing*, vol. 1, 1997, pp.575–578.

[5] L. Yu and L. B. White, "Optimum receiver design for broadband Doppler compensation in multipath/doppler channels with rational orthogonal wavelet signalling," *IEEE Trans. Signal Processing*, vol. 55, no. 8, pp. 4091–4103, Aug. 2007.

[6] N. Owsley and G. Swope, "Time delay estimation in a sensor array," *IEEE Trans. Acoustics, Speech and Signal Processing*, vol. 29, pp. 519–523, 1981.

[7] A. Zajic, "Statistical modeling of mimo mobile-to-mobile underwater channels," *IEEE Trans. Vehicular Technology*, vol. 60, pp. 1337–1351, 2011.

[8] P. Auscher, "Wavelet bases for L2(R) with rational dilation factor," *Wavelets and Their Applications, Boston Jones and Barlett*, pp. 439– 451, 1992.

[9] L. Yu and L. B. White, "Complex rational orthogonal wavelet and its application in communications," *IEEE Sig. Proc. Letters*, vol. 13, no. 8, pp. 477–480, Aug. 2006.

[10] S. Mallat, Ed., *A Wavelet Tour of Signal Processing*. Oxford, UK: Academic Press, 1999.

[11] G. Strang and T. Nguyen, Eds., *Wavelets and Filter Banks*. Wellesley MA USA: Wellesley-Cambridge Press, 1996.

[12] P. Duilleux, "An implementaton of the algorithm à trous to compute the wavelet transform." in *Wavelet: Time-Frequency Methods and Phase Spaces*, Berlin: Springer, IPTI: Oxford Univ. Press, 1989.

[13] M. Unser, A. Aldroubi, and S. J. Schiff, "Fast implementation of the continous wavelet transform with integer scales," *IEEE Trans. Signal Processing*, vol. 42, no. 12, pp. 3519–3523, 1994.

[14] M. Shensa, "The discrete wavelet transform: wedding the à trous and mallat algorithms," *IEEE Trans. Signal Processing*, vol. 40, pp. 2464–2482, 1992.

[15] O. Rioul and P. Duhamel, "Fast algorithms for discrete and continuous wavelet transforms," *IEEE Trans. Information Theory*, vol. 38, pp. 569–586, 1992.

[16] A. Baussard, F. Nicolier, and F. Truchetter, "Rational multiresolution analysis and fast wavelet transform: Application to wavelet shrinkage denoising," *Signal Processing 84, ELSEVIER*, pp. 1735–1747, 2004.

[17] M. Vetterli and T. T. Verma. Filterbank implementation of meyer's wavelet. [Online]. Available: http://www.stanford.edu/ dattorro/Wavelet.pdf

[18] C. K. Chui, *An Introduction to Wavelets*, Academic Press, New York, 1992.

[19] P. P. Vaidyanathan, *Multirate Systems and Filter Banks*, Prentice Hall, 1993.

[20] J. Kovacevic and M. Vetterli, "Perfect reconstruction filter banks with rational sampling factors," *IEEE Trans. Sig. Proc.*, vol. 41, no. 6, pp. 2047–2066, June 1993

Limin Yu (M'12) received the B.Eng. and M.Sc. degrees of Communications Engineering from Xiamen University, Xiamen, China, in 1999 and 2002 respectively. She received the PhD degree of Telecommunications engineering from the University of Adelaide, Adelaide, Australia, in 2007. She was with the National Key Laboratory of Underwater Acoustic Communications in Xiamen University from 1999 to 2002. From 2002 to 2003, she worked at the 3G Development Group, Software Support Division, ZTE Telecommunication Co. Ltd, Shenzhen, China. She was a postdoctoral researcher at the University of South Australia and the University of Adelaide from 2007 to 2012. She is currently a lecturer at the Xi'an Jiaotong-Liverpool University, Suzhou, China. Her research interests include wavelet and filer banks, statical inference and signal processing theory with applications in underwater acoustic communications, sonar detection, broadband systems, sensor networks and medical image analysis.

Fei Ma received the B.Sc. (Math) and M.Sc.(Math) degrees from Xiamen University, Xiamen, China, in 1999 and 2002 respectively. He received the PhD of Applied Mathematics from Flinders University, Australia, in 2009. From 2002 to 2004, he worked as a software engineer for Kingdee Software China Co. Ltd. He stayed in Flinders University after he finished the PhD study and worked as a research associate. From 2009 to 2012, he was an analyst in Symbion, Australia. Currently he is a lecturer at Xi'an Jiaotong-Liverpool University, Suzhou, China. His research interests include medical image analysis and matrix theory.

Langford B. White (SM'00) received the B.Sc. (Math.), B.E.(Hons.), and Ph.D. (Elect. Eng.) degrees from the University of Queensland, Brisbane, Australia, in 1984, 1985, and 1989 respectively. From 1986 to 1999, he worked for the Defence Science and Technology Organization, Salisbury, Australia. Since 1999, he has been a Professor with the School of Electrical and Electronic Engineering, The University of Adelaide, Adelaide, Australia, where he is also Director of the Centre for Internet Technology Research. His research interests include signal processing, control, telecommunications, and internet engineering.